Journal of Dentistry 82 (2019) 45–55

Contents lists available at ScienceDirect

Journal of Dentistry

journal homepage: www.elsevier.com/locate/jdent

Biological, mechanical and adhesive properties of universal adhesives containing zinc and copper nanoparticles

Mario F. Gutiérrez[a,b], Luisa F. Alegría-Acevedo[a], Luján Méndez-Bauer[a], Jorge Bermudez[a], Andrés Dávila-Sánchez[a,c], Sonja Buvinic[b], Nadia Hernández-Moya[b], Alessandra Reis[a], Alessandro D. Loguercio[a], Paulo V. Farago[d], Javier Martin[e], Eduardo Fernández[e,f,*]

[a] Department of Restorative Dentistry, School of Dentistry, State University of Ponta Grossa, Rua Carlos Cavalcanti, 4748, Zip Code 84030-900, Campus Uvaranas, Ponta Grossa, Paraná, Brazil
[b] Institute for Research in Dental Sciences, Faculty of Dentistry, University of Chile, Av. Sergio Livingstone Pohlhammer 943, Zip Code 7500566, Independencia, Santiago, Chile
[c] Department of Restorative Dentistry and Biomaterials, San Francisco de Quito University, Av. Diego de Robles y Vía Interoceánica, Zip Code 170901, Quito, Ecuador
[d] Department of Pharmaceutical Sciences, State University of Ponta Grossa, Rua Carlos Cavalcanti, 4748, Zip Code 84030-900, Campus Uvaranas, Ponta Grossa, Paraná, Brazil
[e] Department of Restorative Dentistry, Faculty of Dentistry, University of Chile, Sergio Livingstone Pohlhammer 943, Zip Code 7500566, Independencia, Santiago, Chile
[f] Instituto de Ciencias Biomédicas, Universidad Autónoma de Chile, Av. Pedro de Valdivia 425, Zip Code 7500912, Providencia, Santiago, Chile

ARTICLE INFO

Keywords:
Universal adhesive system
Zinc oxide
Copper
Nanoparticles
Microtensile bond strength and nanoleakage

ABSTRACT

Objectives: To evaluate the effect of addition of zinc oxide and copper nanoparticles (ZnO/CuNp) into universal adhesives, on antimicrobial activity (AMA), cytotoxicity (CTX), water sorption (WS) and solubility (SO), microhardness (MH) and *in vitro* degree of conversion (DC), as well as resin-dentin microtensile bond strength (μTBS), nanoleakage (NL) and *in situ* DC.

Methods: ZnO/CuNp (0% [control]; 5/0.1 and 5/0.2 wt%) were added in Prime&Bond Active (PBA) and Ambar Universal (AMB). The AMA was evaluated against *Streptococcus mutans*. For CTX, Saos-2 cell-line was used. For WS and SO, specimens were tested for 28d. For MH, specimens were tested after 24 h and 28d and for *in vitro* DC, specimens were evaluated after 24 h. After, the adhesives were applied to flat dentine surfaces, composite resin build-ups, specimens were sectioned to obtain resin–dentine sticks. It was evaluated in μTBS, NL and *in situ* DC after 24 h of water storage. ANOVA and Tukey's test were applied ($\alpha = 0.05$).

Results: The addition of 5/0.2 ZnO/CuNp increase AMA and WS, but decrease the SO when compared to control ($p < 0.05$). The CTX and μTBS were maintaining with adhesive-containing ZnO/CuNp ($p > 0.05$). MH, *in vitro* DC and *in situ* DC was significant increase (AMB) or maintaining (PBA) with ZnO/CuNp addition. However, significantly lower NL was observed for ZnO/CuNp groups ($p < 0.05$).

Conclusions: The addition of ZnO/CuNp in the tested concentrations in universal adhesive systems may be an alternative to provide antimicrobial activity and improves the integrity of the hybrid layer, without jeopardizing biological, adhesives and mechanical properties.

Significance: This is the first study that demonstrates that the addition of zinc oxide and copper nanoparticles in concentrations up to 5/0.2 wt% in two universal adhesive systems is a feasible approach and may be an alternative to adhesive interfaces with antimicrobial properties and less defects in the resin-dentin interface.

1. Introduction

Composite resins are increasingly gaining more space in restorative dentistry, offering such advantages as aesthetics and less invasive preparation techniques [1,2]. However, the lack of durable dental adhesives and secondary caries are considered one of the main problems with contemporary adhesive restorations, negatively affecting their clinical success [2,3]. On the other hand, removal of composite resins leads to loss sound tooth structure, increasing cavity volume and needing a more complex restoration [4]. Thus, this reduced longevity

* Corresponding author at: Department of Restorative Dentistry, Faculty of Dentistry, University of Chile, Sergio Livingstone Pohlhammer 943, Independencia and Instituto de Ciencias Biomédicas, Universidad Aut ónoma de Chile, Pedro de Valdivia 425, Providencia, Santiago, Chile.
E-mail address: efernand@odontologia.uchile.cl (E. Fernández).

https://doi.org/10.1016/j.jdent.2019.01.012
Received 23 November 2018; Received in revised form 16 January 2019; Accepted 21 January 2019

and replacement of these restorations for more complex ones results in millions of dollars spent annually on dental care [5,6].

Thus, the adhesive/dentin interface can be considered the weak link in the composite restoration [3]. Two factors related to adhesive/dentin interface degradation are highlighted: the hydrolytic degradation over time of the polymer present in the hybrid or adhesive layers, and a poorly infiltrated hybrid layer with unprotect collagen fibers, that could be hydrolyzed by host-derived matrix metalloproteinase (MMPs) and cysteine cathepsines (CTs) [7,8]. These enzymes are activated by pH changes relevant to acid etching process and/or by an acidic pH brought about by lactate release from cariogenic bacteria, indicating the role of bacterial acids in the process [9,10]. This is why the development of materials with antibacterial and MMPs/CTs inhibitors properties becomes so important, in order to increase the durability of the adhesive/dentin interface, without compromising the mechanical properties of the adhesive formation [11,12].

In recent years, metallic nanoparticles have been highlighted among the most promising agents with antibacterial properties, which exhibit biocidal activities at exceptionally low concentrations [13]. In this sense, copper nanoparticles (CuNp) have been shown to be effective against gram-positive and gram-negative bacteria [14]. In addition to important antimicrobial activity, copper is cheap, so the synthesis of copper nanoparticles has a better cost-benefit ratio. Also, CuNp seems to be a potent inhibitor of MMPs. Several studies showed that copper has the ability to inhibit the dentin MMP-2, and to stimulate the secretion of tissue inhibitors of MMPs (TIMPs), causing lower degradation pattern in the resin/dentine interface [15,16]. Otherwise, zinc oxide nanoparticles (ZnONp) can promote subtle conformational in collagenase cleavage sites in collagen molecules that protects collagen from MMP's activity [17].

Recent studies showed that the addition of CuNp in concentrations up to 0.1 wt% in an adhesive system provides antimicrobial properties and preserves the bonding to dentin after 1 and 2-year of water storage, without reducing the mechanical properties of the adhesive formulations [18,19]. Likewise, the incorporation of ZnONp in an adhesive system preserves the bonding to dentin after 6-month, without reducing the mechanical properties of the adhesive [20]. Moreover, formulations also resulted in the formation of apatite crystallites on the collagen fibrils, favoring dentin mineralization, reducing MMPs-mediated collagen degradation [17,21], may inhibit dentin demineralization [22], and may promote enamel remineralization [23].

Nevertheless, the effect of combining of ZnONp and CuNp in the same adhesive system has not been studied, as well as, the properly concentration of each one. This is necessary, because any change in the well-balanced chemical composition of adhesive systems could imply possible mechanical and physico-chemical failures and biological hazards [20].

Therefore, we designed this *in vitro* study to investigate the effect of adding different concentrations of zinc oxide and copper nanoparticles (ZnO/CuNp) into two commercial universal adhesive systems on the antimicrobial activity, cytotoxicity, water sorption and solubility, microhardness, *in vitro* degree of conversion, as well as immediate resin-dentine microtensile bond strength, nanoleakage and *in situ* degree of conversion.

2. Materials and methods

2.1. Characterization of zinc oxide and copper nanoparticles

The ZnONp and CuNp (SkySpring Nanomaterials, Inc., Houston, TX, USA; www.ssnano.com) were characterized by field emission scanning electron microscope (FE-SEM), atomic force microscopy (AFM), and energy dispersive X-ray (EDX) analysis. The ZnONp and CuNp nanoparticles properties are shown in Table 1.

Table 1
Zinc oxide and Copper Nanoparticles Specifications.

Type of particles/batch number/ manufacturer	Specifications
Zinc oxide nanoparticles (ZnO) 8410DL Skyspring Nanomaterials, Inc*	Purity: 99.8% trace metals basis Appearance: White-yellow nanopowder APS: 10-30 nm SSA: 30-50 m^2/g
Copper nanoparticles (Cu) 0820XH Skyspring Nanomaterials, Inc*	Purity: 99.9% trace metals basis Appearance: Black nanopowder APS: 40-60 nm SSA: ~12 m^2/g Morphology: spherical Bulk density: 0.19 g/cm^3 True density: 8.9 g/cm^3

APS, Average Particle Size; SSA: Specific Surface Area.
(*) www.ssnano.com.

2.2. Formulation of the experimental adhesives

We formulated experimental adhesives using two universal adhesive systems: Prime&Bond Active (Dentsply-Sirona, Konstanz, Baden-Württemberg, Germany) and Ambar Universal (FGM Prod. Odont. Ltda, Joinville, SC, Brazil). Six experimental adhesives systems were formulated according to the addition of different concentrations of ZnO/CuNp for each commercial universal adhesive (wt%): 0% (control, commercial material); 5% zinc and 0.1% copper (5/0.1); 5% zinc and 0.2% copper (5/0.2). These concentrations were used based on previous literature [18–21] and results from a pilot study (not showed data). The incorporation to the adhesive solution was done in a dark room with a motorized stirrer [19].

2.3. Antimicrobial activity

Pure culture was obtained by culturing *Streptococcus mutans* (*S. mutans)* ATCC 25175 in brain heart infusion (BHI) broth (Difco Laboratories, Detroit, MI, USA) for 72 h at 37 °C [19]. Then, 100 µL of the bacterial suspension was swabbed onto BHI agar plates (Difco Laboratories, Detroit, MI, USA) to create the lawn [24]. Disk diffusion method was used to measure *S. mutans* sensitivity to the adhesive groups (described above) and to an aqueous solution of nanoparticles in the same concentrations described for the experimental adhesives (0% [control, distilled water]; 5/0.1 and 5/0.2). Filter paper discs of 5 mm diameter were prepared from Whatman filter paper No. 1, placed in a petri dish and sterilized in a hot air oven at 160 °C for 2 h. Thereafter, discs were impregnated according to the following: 1) with 20 µL of each of the aqueous solution and placed immediately over the plates and; 2) with 20 µL of each of the experimental adhesive, evaporating the solvent and light-cured for 20 s with a LED light source at 1000 mW/cm^2 (VALO, Ultradent Products, South Jordan, UT, USA), and placed immediately over the plates.

The plates were incubated in an anaerobic jar (5% CO_2) for 48 h at 37 °C. The inhibition zones (mm) were measured with a digital caliper to the nearest 0.1 mm (Absolute Digimatic, Mitutoyo, Tokyo, Japan). Three samples of each adhesive groups and aqueous solution were tested.

2.4. In vitro cytotoxicity

2.4.1. Cell culture

Osteoblast-like cell line Saos-2 (ATCC® HTB-85™) was used for determination of cytotoxicity of adhesive groups and only nanoparticles in an aqueous solution such described for antimicrobial activity test. Saos-2 cells were cultured in Dulbecco's Modified Eagle's Medium (DMEM; Thermo Fisher Scientific, Dreieich, Germany) supplemented with 10%

Fetal Bovine Serum (FBS; BI Biological Industries) and 1% penicillin-streptomycin solution (Thermo Fisher Scientific), in a humidified atmosphere containing 5% CO_2 and 95% air at 37 °C [25]. Medium was changed every 2–3 days. After reaching confluence the cells were washed with Dulbecco's phosphate buffered saline (PBS; Thermo Fisher Scientific) and detached with trypsin-EDTA 0.05% for 5 min (Thermo Fisher Scientific). A cell fraction was stained with a trypan blue solution (Sigma–Aldrich, Munich, Germany) and counted in a hemocytometer, for then plating the desired cell number.

2.4.2. Cell stimulation

All stimulation experiments were performed in 96-well plates in triplicate. All experiments were repeated for at least three times. In brief, we seeded 10,000 cells per well, that render a 70% confluence 24 h after seeding. Cells were incubated with three different dilutions (1, 0.1, and 0.01 v/v%) of adhesive groups and aqueous solutions in 100 µl cell culture medium for 24 h at 37 °C [25]. Incubation with plain culture medium was used as 100% viability control, while 20% methanol was used as an apoptosis control.

2.4.3. Assessment of cytotoxicity using MTT assay

Cell cytotoxicity was determined using the Vybrant® MTT Cell Proliferation Assay Kit (Thermo Fisher Scientific). After stimulation for 24 h, the medium was removed and replaced with 100 µL of fresh culture medium. Ten µL of 12 mM MTT stock solution (prepared according to manufacturer´s instructions) were added to each well, and incubate at 37 °C for 2 h. After that, 100 µL of SDS-HCl solution (prepared according to manufacturer´s instructions) were added to each well and thoroughly mixed by pipetting. The microplate was incubated at 37 °C for 4 h, followed by the measurement of absorbance at 490 nm with a 670 nm-correction wavelength in a microplate reader. Cell viability was calculated and normalized to control experiments (=100%).

2.5. Water sorption and solubility

The ISO specification 4049 helped determine water sorption and solubility [26], except for specimens' dimensions. After isolating a metallic matrix (5.8 mm diameter, 1.0 mm thick) with a very thin layer of petroleum jelly, we dispensed the adhesive until completely fill the mold. All visible air bubbles trapped in the adhesive specimens were carefully removed with a brush (Cavibrush, FGM Prod. Odont. Ltda, Joinville, SC, Brazil). An air stream was applied for solvent evaporation for 40 s at a distance of 10 cm.

Under a plastic matrix strip, the adhesive specimens were light-cured for 40 s with a LED light source at 1000 mW/cm^2 (VALO, Ultradent Products, South Jordan, UT, USA), in close contact with each disc-like specimen. After polymerization, the specimens were removed from the mold and polished with 600-grit SiC paper in order to remove the adhesive excesses and the oxygen-inhibition layer. Five adhesive discs of each group were made.

Immediately after polymerization, we placed the specimens in desiccators, transferred them to a pre-conditioning oven at 37 °C, and left them undisturbed for 5 days. After that, we weighed them at 24 h intervals until the daily variation of mass dropped below 0.2 mg ($m1$). A digital caliper measured specimens' thickness and diameter (Absolute Digimatic, Mitutoyo) for calculation of the volume (V) of each specimen in mm^3. Ten specimens were produced for each group.

We then placed each specimen in a sealed Eppendorf containing 10 mL of distilled water (pH 7.2) at 37 °C. After fixed time intervals of 1 to 8 h, and 1 to 7, 14, and 28 days of storage, we removed the Eppendorfs from the oven and left them at room temperature for 30 min. The specimens were washed in running water, gently wiped with a soft absorbent paper and weighed in an analytical balance ($m2$). After that, they were returned to the vials with 10 mL of fresh water. After the 28-day storage time, desiccators containing fresh silica gel in an oven dried the specimens at 37 °C, where they remained undisturbed for 5 days or until the daily weighing variations dropped below 0.2 mg. At this moment, the specimens were weighted again in an analytical balance ($m3$). The initial mass determined after the first desiccation process ($m1$) was used to calculate the change in mass after each fixed time interval, during the 28 days of storage in water. Changes in mass were plotted against the storage time in order to obtain the kinetics of water absorption during the entire period of water storage.

Water sorption and solubility over the 28 days of water storage were calculated using the following formula: Water sorption = $(m2 - m3)/V$ and Solubility = $(m1 - m3)/V$.

2.6. Knoop microhardness

Five adhesive discs of each group were produced as described for water sorption and solubility test. After preparation, specimens were stored in a dark vial for 24 h and 28 days before microhardness measurement. Specimens were then taken to an HMV-2 microhardness tester (Shimadzu; Tokyo, Japan) equipped with a Knoop indenter. Five measurements were performed of each specimen with a load of 10 g for 15 s. The first measurement was performed in the center of the adhesive disc. The other four measurements were performed 100 µm and 200 µm to the left and right of the first one. Values obtained for the same specimen were averaged for statistical purposes.

2.7. In vitro degree of conversion

Ten new adhesive discs of each group were produced as described water sorption and solubility test. Specimens were stored in a wet environment for 24 h at 37 °C prior to performing the DC readings. The DC measurements were performed in a micro-Raman spectrometer (Bruker Optik GmbH, Ettlingen, Baden-Württemberg, Germany).

The micro-Raman spectrometer was first calibrated for zero and then for coefficient values using a silicon specimen. Specimens were analyzed using the following micro-Raman parameters: 20-mW Neon laser with 532-nm wavelength, spatial resolution of ≈ 3 µm, spectral resolution ≈ 5 cm^{-1}, accumulation time of 20 s with 6 co-additions, and magnification of 20x (Olympus UK, London, UK) to beam diameter of ≈ 1 µm [47,48]. The spectra were taken at three different sites for each specimen and the values averaged for statistical purposes. Spectra of uncured adhesives were taken as reference. Post-processing of spectra was performed using the dedicated Opus Spectroscopy Software version 6.5 (Bruker Optik GmbH, Ettlingen, Baden- Württemberg, Germany).

The ratio of the double-bond content of monomer to polymer in the adhesive was calculated according to the following formula: DC (%) = $(1 - R_{cured}/R_{uncured})$ x 100, where R is the ratio of aliphatic and aromatic peak areas at 1639 cm^{-1} and 1609 cm^{-1} in cured and uncured adhesives.

2.8. Teeth preparation and bonding procedures

Sixty caries-free extracted human third molars, collected from patients with age ranging from 18 to 35 years old were used. The teeth were collected after the patient's informed consent. The Ethics Committee approved this study under protocol number 2.399.496. Teeth were disinfected in 0.5% chloramine, stored in distilled water and used within 3 months after extraction. A flat dentin surface was exposed on each tooth after wet grinding the occlusal and surrounding enamel with 180-grit SiC paper. The enamel-free, exposed dentin surfaces were further polished with 600-grit silicon-carbide paper for 60 s to standardize the smear layer.

The adhesives were applied at etch-and-rinse (ER) or self-etch (SE) mode, as per manufacturer' instructions (Table 2). In ER mode, the dentine surface was acid etched with 37% phosphoric acid for 15 s (Condac, FGM Prod. Odont. Ltda, Joinville, SC, Brazil), water rinsed for 15 s and dried with absorbent paper keeping the dentin surface slightly

Table 2
Universal adhesive system (batch number), composition (*) and application mode.

Universal adhesive system (batch number) and pH	Composition (*)	Etch-and-rinse mode	Self-etch mode
Prime&Bond Active (PBA - Dentsply-Sirona, Konstanz, Baden-Württemberg, Germany) (1703000452) pH = ~2,5	Phosphoric acid modified acrylate resin, multifunctional acrylate, bifunctional acrylate, acidic acrylate, isopropanol, water, initiator, Stabilizer (10-MDP and PENTA)	1. Apply phosphoric acid for 15 s. 2. Remove gel with vigorous water spray and rinse conditioned areas thoroughly for 15 s. 3. Remove rinsing water completely by blowing gently with an air syringe or blot dry. Do not desiccate dentin. 4. Apply adhesive to completely wet the surfaces to be treated. If necessary rewet applicator tip. Avoid pooling of the adhesive. 5. Keep the adhesive slightly agitated for 20 seconds. 6. Disperse adhesive and remove solvent with clean, dry air from an air-water syringe. Treat every surface with a moderate air flow for at least 5 seconds until a glossy and uniform layer results. 7. Light cure for 10 s at 1200 mW/cm^2	1. Apply adhesive to completely wet the surfaces to be treated. If necessary rewet applicator tip. Avoid pooling of the adhesive. 2. Keep the adhesive slightly agitated for 20 seconds. 3. Disperse adhesive and remove solvent with clean, dry air from an air-water syringe. Treat every surface with a moderate air flow for at least 5 seconds until a glossy and uniform layer results. 4. Light cure for 10 s at 1200 mW/cm^2
Ambar Universal (AMU - FGM Prod. Odontológicos, Joinville, Santa Catarina, Brazil) (310516) pH = 2,6 - 3,0	10-MDP, methacrylic monomers, photoinitiators, coinitiators, stabilizers, silica nanoparticles and ethanol	1. Apply phosphoric acid for 15 s. 2. Wash the surface with plenty of water and dry the cavity so that the dentin does not get dehydrated, but without the accumulation of water on the surface. 3. Apply a first layer vigorously rubbing the adhesive with the micro applicator for 10 s. 4. Next, apply a second layer of adhesive for 10 s, spreading the product. 5. Evaporate excess solvent by thoroughly air-drying with an air syringe for 10 s 6. Light cure for 10 s at 1200 mW/cm^2	1. Apply a first layer vigorously rubbing the adhesive with the micro applicator for 10 s. 2. Next, apply a second layer of adhesive for 10 s, spreading the product. 3. Evaporate excess solvent by thoroughly air-drying with an air syringe for 10 s 4. Light cure for 10 s at 1200 mW/cm^2

(*) 10-MDP = methacryloyloxydecyl dihydrogen phosphate; PENTA = dipentaerythritol penta acrylate monophosphate.

wet. After the bonding procedures, resin composite blocks (Opallis, FGM Prod. Odont. Ltda, Joinville, SC, Brazil) were buildup on the bonded surfaces in 3 increments of 1.0 mm thick each and each one was individually light activated for 40 s. A single operator carried out all bonding procedures in an environment with controlled temperature and humidity. Five teeth were used for each experimental group.

After storage of the bonded teeth in distilled water at 37 °C for 24 h, they were longitudinally sectioned in both "x" and "y" directions across the bonded interface with a diamond saw in a cutting machine (IsoMet 1000; Buehler, Lake Bluff, USA), under water cooling at 300 rpm to obtain resin-dentine sticks with a cross-sectional area of approximately 0.8 mm^2. The number of premature failures (PF) per tooth during specimen preparation was recorded. The cross-sectional area of each stick was measured with the digital caliper to the nearest 0.01 mm and recorded for subsequent calculation of the microtensile bond strength values (Absolute Digimatic, Mitutoyo, Tokyo, Japan). The resin-dentin sticks from each tooth were then divided as follow:

- Two sticks were used for nanoleakage evaluation.
- Two sticks were used to measure the immediate *in situ* degree of conversion.
- The remaining sticks were submitted to microtensile bond strength test.

2.9. Microtensile bond strength testing

Each stick was attached to a modified device for microtensile bond strength test with cyanoacrylate resin (IC-Gel, bSi Inc., Atascadero, CA, USA) and subjected to a tensile force in a universal testing machine (Kratos, São Paulo, SP, Brazil) at 0.5 mm/min. The failure mode was evaluated under an optical microscope (SZH-131, Olympus; Tokyo, Japan) at 40x and classified as cohesive in dentin (failure exclusive within cohesive dentin – CD); cohesive in resin (failure exclusive within cohesive resin – CR); adhesive (failure at resin/dentin interface – A), or mixed (failure at resin/dentin interface that included cohesive failure of the neighboring substrates, M). The number of premature failures (PF) was recorded and it was not included in the average mean bond strength.

2.10. Nanoleakage evaluation

Before performing the nanoleakage test, a pilot test was conducted to evaluate if the presence of zinc and copper in the adhesive could impair the visualization of silver nitrate uptake. For this purpose, we performed scanning electron microscopy (SEM) images of resin-dentin interfaces of all groups without immersion in silver nitrate. Even in adhesive interfaces with the highest zinc (5%) or copper (0.2%) concentration, ZnONp and CuNp were not observed using the same parameters described above. And thus, the results of nanoleakage test reflect the amount of silver uptake into unpolymerized areas and/or nanospaces not infiltrated by the resin adhesive but not the presence of zinc or copper in the hybrid layer.

After this preliminary test, all resin-dentin sticks selected for this test were coated with two layers of nail varnish applied up to within 1 mm of the bonded interfaces. The resin-dentin sticks were immersed in 50 wt% ammoniacal silver nitrate solution in total darkness for 24 h, rinsed thoroughly in distilled water, and immersed in photo developing solution for 8 h under a fluorescent light to reduce silver ions into

metallic silver grains within voids along the bonded interface.

Specimens were mounted on aluminum stubs, polished with 1000-, 1500-, 2000- and 2500-grit SiC paper and 1 and 0.25 μm diamond paste (Buehler Ltd., Lake Bluff, IL, USA). Then, they were ultrasonically cleaned, air dried and gold sputter coated (MED 010, Balzers Union, Balzers, Liechtenstein). The interfaces were observed in a scanning electron microscope in the backscattered mode at 15 kV (VEGA 3 TESCAN, Shimadzu, Tokyo, Japan).

In a way to standardize image acquisition, three pictures were taken of each specimen. The first picture was taken in the center of the resin-dentin stick. The other two pictures were taken 0.3 mm to the left and right of the first one. As two resin-dentin sticks per tooth were evaluated and a total of five teeth were used for each experimental condition, a total of 30 images were evaluated per group. A technician who was blinded to the experimental conditions under evaluation took them all. The relative percentage of nanoleakage within the adhesive and hybrid layer areas was measured in all pictures using the public domain Image J software, a Java-based image processing software package developed at the National Institutes of Health (NIH) [27].

2.11. In situ degree of conversion within adhesive/hybrid layers

All resin-dentin sticks selected for this test were wet polished using 1500; 2000; 2500 and 4000-grit SiC paper for 30 s each. The specimens were ultrasonically cleaned for 10 min and positioned into micro-Raman equipment. The DC measurements were performed in a micro-Raman spectrometer (Bruker Optik GmbH, Ettlingen, Baden-Württemberg, Germany). The micro-Raman spectrometer was first calibrated for zero and then for coefficient values using a silicon specimen. Specimens were analyzed using the following micro-Raman parameters: 20-mW Neon laser with 532-nm wavelength, spatial resolution of ≈ 3 μm, spectral resolution ≈ 5 cm^{-1}, accumulation time of 30 s with 6 co-additions, and magnification of 100x (Olympus UK, London, UK) to beam diameter of ≈ 1 μm. The spectra were taken at the resin-dentin interface, in the middle of the hybrid layer within the intertubular dentin, at three different sites for each specimen and the values averaged for statistical purposes. Spectra of uncured adhesives were taken as reference. Post-processing of spectra was performed using the dedicated Opus Spectroscopy Software version 6.5 (Bruker Optik GmbH, Ettlingen, Baden-Württemberg, Germany). The ratio of the double-bond content of monomer to polymer in the adhesive was calculated according to the formula described earlier in the materials and methods section in the item *in vitro* degree of conversion.

2.12. Statistical analysis

The data were first analyzed using the Kolmogorov-Smirnov test to assess whether the data followed a normal distribution, as well as Barlett's test for equality of variances to determine if the assumption of equal variances was valid. After confirming the normality of the data distribution and the equality of the variances, data for the microbiological test (mm), cytotoxicity, water sorption and solubility, *in vitro* degree of conversion (%) were subjected to a one-way ANOVA. Data for microhardness (KNH) was subjected to a two-way ANOVA. The μTBS (MPa), nanoleakage (%) and *in situ* degree of conversion (%) data of each adhesive were subjected to one-way ANOVA. Tukey's post hoc test was used for pair-wise comparisons ($\alpha = 0.05$) using the Statistica for Windows software (StatSoft, Tulsa, OK, USA).

3. Results

3.1. Characterization of zinc oxide and copper nanoparticles

The FE-SEM and AFM (Fig. 1) confirm that the zinc oxide and copper particles have a nanometer size. As demonstrated in the EDX spectrum of a representative specimen (Fig. 2), the samples have a high percentage of zinc (a) and copper (b) atoms, without contamination with other elements.

3.2. Antimicrobial activity

The results of antimicrobial activity against *S. mutans* of the different concentrations of ZnO/CuNp, incorporated in distilled water and in universal adhesives systems, are shown in Table 3. For aqueous solution, all ZnO/Cu-containing solutions showed antibacterial properties against *S. mutans* significantly higher than control ($p = 0.001$). For both universal adhesives, only 5/0.2 groups showed antibacterial properties against *S. mutans* significantly higher than respective control ($p < 0.05$).

3.3. In vitro cytotoxicity

When the ZnO/CuNp were diluted in distilled water, only the 5/0.2 group showed a high cytotoxicity when compared to the control (distilled water) in the three dilutions (Fig. 3A; 1 ($p < 0.01$), 0.1 ($p < 0.05$), and 0.01 v/v% ($p < 0.05$) respectively). No differences were observed between dilutions (Fig. 3A; $p > 0.05$). When compared with the viability control (culture medium), no differences were observed in all groups (Fig. 3A; $p > 0.05$)

When the ZnO/CuNp were incorporated into the Prime&Bond Active adhesive, significantly higher cytotoxicity was observed between 5/0.1 and 5/0.2 group when compared to the control (commercial material) only at the dilution of 0.01 v/v% (Fig. 3B; $p < 0.001$). Dilutions 0.1 and 1 v/v% showed more cytotoxicity when compared to 0.01 v/v% dilution, in all adhesive groups (Fig. 3B; $p < 0.001$). When compared with the viability control (culture medium), dilutions 0.1 and 1 v/v% showed more cytotoxicity in all adhesive groups (Fig. 3B; $p < 0.05$)

When the ZnO/CuNp were incorporated into the Ambar Universal adhesive, none differences in cytotoxicity were observed between the ZnO/CuNp concentrations and the control (commercial material) and any of the tested dilutions (Fig. 3C; $p > 0.05$). Dilutions 1 and 0.1 v/v % showed more cytotoxicity when compared to 0.01 v/v% dilution, in all adhesive groups (Fig. 3C; $p < 0.001$). When compared with the viability control (culture medium), dilutions 1 and 0.1 v/v% showed more cytotoxicity in all adhesive groups (Fig. 3C; $p < 0.01$).

3.4. Water sorption and solubility

When the ZnO/CuNp were incorporated into the Prime&Bond Active adhesive, for the 28-day cumulative water sorption, significant higher water sorption was detected in 5/0.1 and 5/0.2 group when compared to control (Table 4; $p = 0.001$). For solubility, only the 5/0.2 group showed significantly higher solubility than control (Table 4; $p < 0.05$).

When the ZnO/CuNp were incorporated into the Ambar Universal adhesive, only the 5/0.2 group showed significantly higher 28-day cumulative water sorption than control (Table 4; $p < 0.01$). All ZnO/CuNp-containing Ambar Universal adhesives showed significantly lower solubility than control (Table 4; $p = 0.001$).

3.5. Knoop microhardness

When the ZnO/CuNp were incorporated into the Prime&Bond Active adhesive, no significant differences among different groups were detected (Table 5; $p = 0.63$). When the ZnO/CuNp were incorporated into the Ambar Universal adhesive, groups with ZnO/CuNp showed higher Knoop microhardness values than control, after 24 h and 28-days (Table 5; $p < 0.01$).

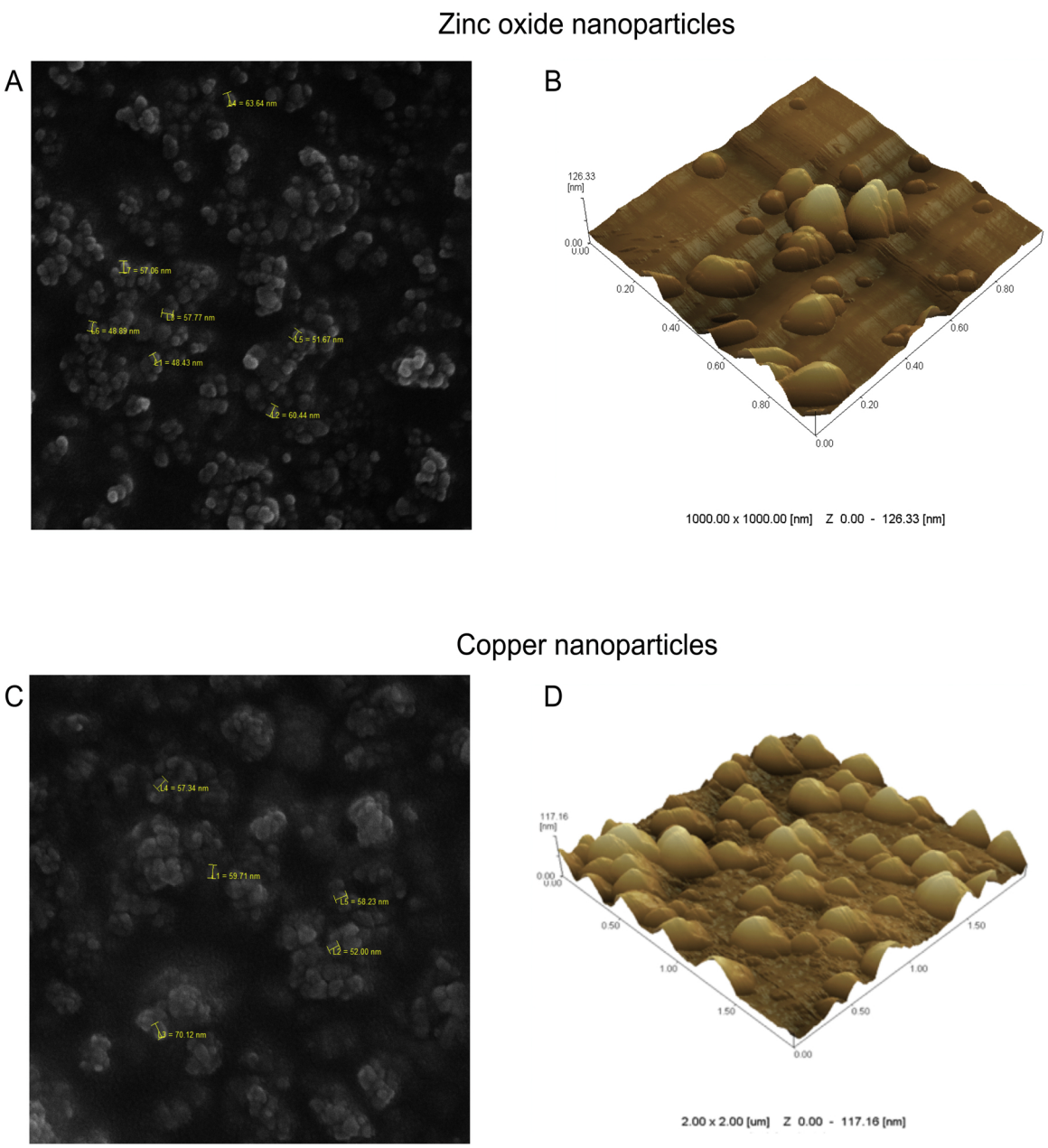

Fig. 1. Field emission scanning electron microscopy (FE-SEM) (A and C) and atomic force microscopy (AFM) (B and D) of the zinc oxide and copper nanoparticles, demonstrating its nanometer size.

3.6. *In vitro* degree of conversion

For *in vitro* degree of conversion, no significant differences among different groups were detected when the ZnO/CuNp were incorporated into the Prime&Bond Active adhesive (Table 5; $p = 0.76$). When the ZnO/CuNp were incorporated into the Ambar Universal adhesive, a significant higher *in vitro* degree of conversion values were observed when compared to control (Table 5; $p < 0.001$).

3.7. *Microtensile bond strength testing*

For both Prime&Bond Active and Ambar Universal adhesive, no significant differences were observed in the microtensile bond strength among all groups, in both adhesive strategies (Fig. 4A and B; $p > 0.05$). The addition of different ZnO/CuNp concentrations did not influence the microtensile bond strength.

3.8. *Nanoleakage evaluation*

For Prime&Bond Active and Ambar Universal, it was observed that the addition of ZnO/CuNp showed lower nanoleakage values than control, in both adhesive strategies (Fig. 4C and D; $p < 0.001$). No difference between application mode was observed in all groups (Fig. 4C and D; $p > 0.05$) (Fig. 5).

3.9. *In situ degree of conversion within adhesive/hybrid layers*

For *in situ* degree of conversion, no significant differences among different groups and application mode were detected in Prime&Bond Active (Fig. 4E; $p = 0.92$). No differences were showed between adhesive strategies.

For Ambar Universal adhesive, two-way ANOVA showed that adhesive formulations with ZnO/CuNp showed higher degree of conversion values than control in etch-and-rinse (5/0.1 and 5/0.2 groups) and

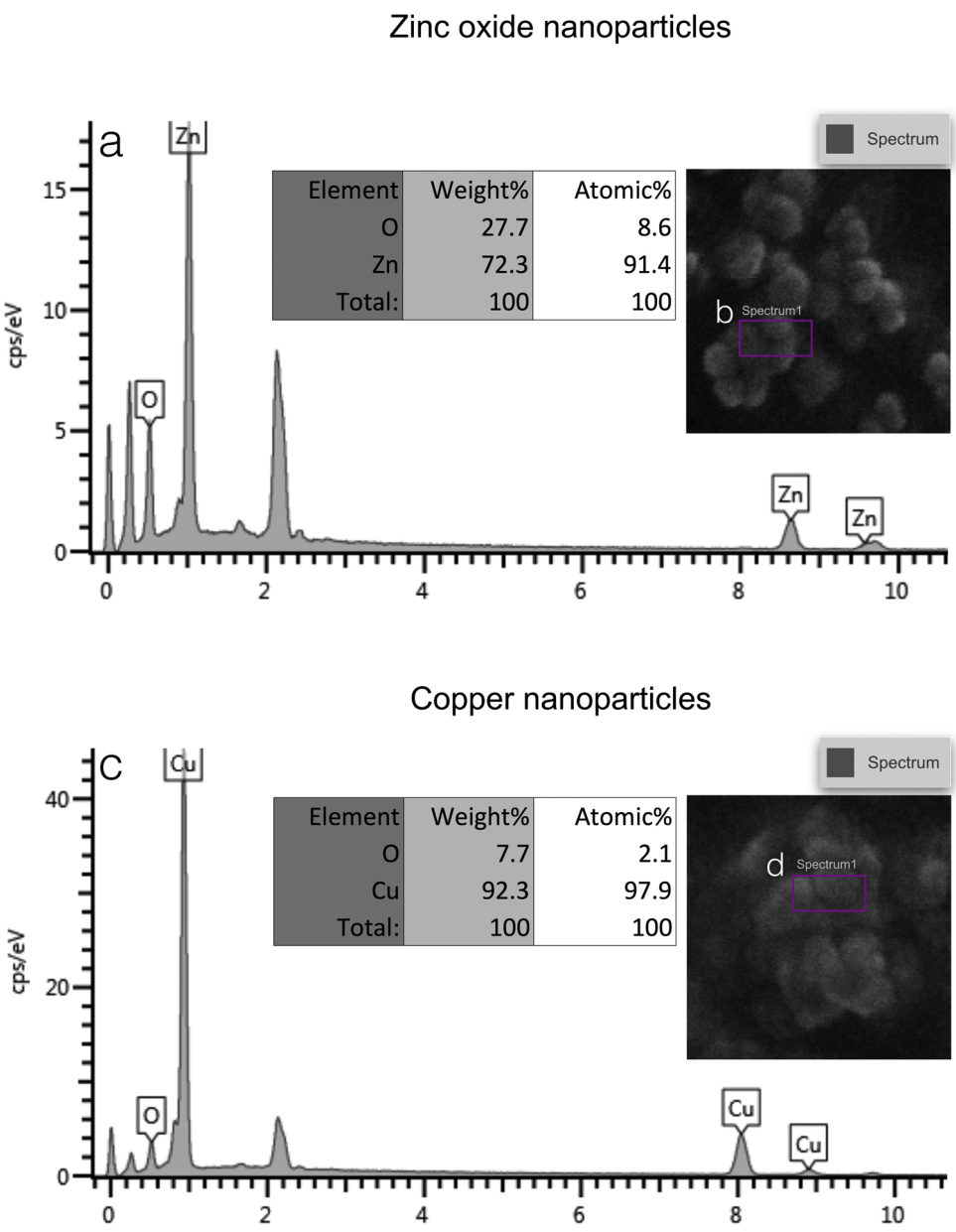

Fig. 2. EDX spectrum (a and c) from selected area of the zinc oxide and copper nanoparticles powder sample outlined by a magenta rectangle in (b) and (d). The figure table summarizes the elemental composition of the sample area outlined.

Table 3
Means and standard deviations of bacterial inhibition halo sizes (mm) against *S. mutans,* obtained in each experimental condition (*).

ZnO/Cu concentration (%)	Aqueous solution	Prime&Bond Active	Ambar Universal
0 (control)	5.73 ± 0.02 ^{A}	6.81 ± 0.54 A	5.71 ± 0.42 a
5 / 0.1	15.77 ± 0.33 ^{B}	7.79 ± 0.50 A,B	6.54 ± 0.43 a,b
5 / 0.2	17.34 ± 1.19 ^{B}	8.64 ± 0.65 B	7.38 ± 0.61 b

(*) Comparisons are valid only within column. Means identified with the same capital, lowercase or uppercase letters are statistically similar. (Tukey´s test, $p \geq 0.05$).

self-etch (5/0.2 group) strategies (Fig. 4F; $p < 0.05$). No differences were showed between adhesive strategies (Fig. 4F; $p > 0.05$).

4. Discussion

The present study was capable to demonstrate that the combination of ZnONp and CuNp present antimicrobial properties against *S. mutans*. Several studies have shown the antimicrobial properties of ZnONp [28] and CuNp [29] as single entities against *S. mutans*, but there is not much evidence on whether the combination improve the effect.

In the present study, for aqueous solution, all ZnO/CuNp combinations (5/0.1 and 5/0.2) showed antibacterial properties against *S. mutans* significantly higher than control, as well as, previously showed to other bacteria [30]. These results suggest that combined metal ions-containing aqueous solutions could have synergistic antibacterial effects. However, the underlying synergistic antibacterial mechanisms of

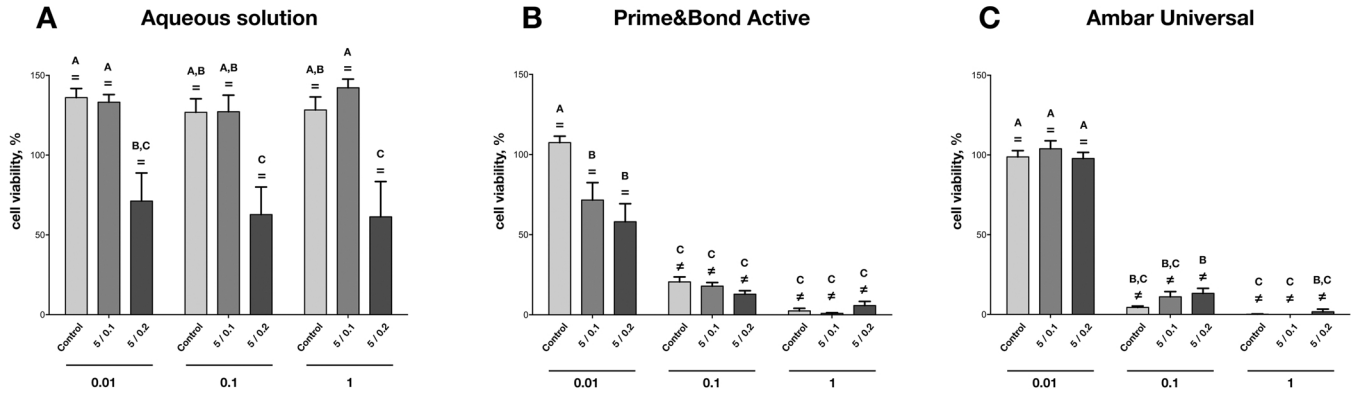

Fig. 3. Cytotoxicity of aqueous solution (A), Prime&Bond Active (B) and Ambar Universal (C) containing zinc oxide and copper nanoparticles in Saos-2 cells. Cells were incubated with three different dilutions (0.01, 0.1, and 1 v/v%) of aqueous solutions and adhesive groups in cell culture medium. Comparisons are valid only within solution/adhesive. Mean ± SEM were calculated. Means identified with the same letter are statistically similar. (Tukey´s test, $p \geq 0.05$). Means identified with equals sign (=) are statistically similar with viability control (100%). (Dunn´s test, $p \geq 0.05$).

the multicomponent metal ions-containing require further investigations.

On the other hand, there are studies that have shown antimicrobial activity against *S. mutans* of dental adhesives incorporating ZnONp [31] and CuNp [18,19]. However, the antimicrobial capacity of ZnO/CuNp combination incorporated in the same dental adhesive has never been evaluated. In the current study, 5/0.2 ZnO/CuNp groups showed antibacterial properties against *S. mutans* significantly higher than respective control, despite being applied on filter paper discs with a thickness of 180 µm, where once polymerized, it could compromise the diffusion capacity of metal ions in that concentration. We believe that this result could reflects faithfully what happens in the clinical practice, simulating the thickness of the adhesive system when applying the adhesive on the dentin surface.

Several mechanisms have been proposed by which the ZnONp and CuNp could exert their antimicrobial effect [13,32,33]. A more recent theory is called "Trojan horse effect", where the acidic lysosomal environment (pH 5.5) is capable of promoting nanoparticles degradation/corrosion, which converts core metals to ions and therefore toxic substances. Also, effect of ZnONp and CuNp do not always depend on the bacteria internalizing the nanoparticles; these nanoparticles can locally change microenvironments near the bacteria and produce reactive oxygen species (ROS) or increase the nanoparticles solubility, which can induce malfunction of other organelles, interactions with –SH groups of key microbial enzymes, leading to denaturation of the bacterial proteins and DNA damage, altering DNA replication of the microorganisms [32,34,35].

In this study, viability of osteoblast-like cell line Saos-2 was tested. Several studies have shown the potential cytotoxicity of ZnONp [36,37] and CuNp [38,39], but little attention has been given to the effects of co-exposure, where nanoparticles of each material may also influence the processes or toxicity caused by the ions released by the other. In this sense, a recent study showed that accumulation of large numbers of ZnONp in human hepatoma cell line HepG2 [40] alters cellular membranes and the cytotoxicity of CuNp is increased. This could explain why group 5/0.2 presented high cytotoxicity when compared to the control (distilled water) in all dilutions.

In the case of adhesive solutions, the viability test is very important because it has been reported that uncured biologically active ingredients of adhesive systems may diffuse across the subjacent dentinal tubules and reach the pulpal tissue, and may modify pulp cell metabolism when the materials are used in deep cavities in spite of a dentin barrier [41,42]. For Prime&Bond Active and Ambar Universal adhesive, all groups showed significantly differences when compared with the viability control (culture medium) in the 1 and 0.1 v/v% dilutions. This can be explained since dental adhesives are highly cytotoxic, due to the monomers in their composition. Several studies have shown the cytotoxic potential of several monomers [25,43]. For instance, Prime&Bond Active and Ambar Universal adhesive contain 10-MDP, which has been shown exerts effects comparable to those of TEGDMA with respect to cytotoxicity, odontoblastic differentiation and inflammatory response in human dental pulp cells [44].

However, some differences were also observed between adhesive systems tested. For Prime&Bond Active, no significant differences were observed in all groups in 0.01 v/v% dilution, when compared with the viability control. However, according to ISO 10993-5 standardization, which mentions that if the viability is reduced to less than 70%, material presents cytotoxic potential [45], 5/0.2 group showed cytotoxicity (58% of cell viability). Moreover, 5/0.1 and 5/0.2 groups showed higher cytotoxicity when compared with control (commercial material). These results could be explained in terms of solubility of Prime&Bond Active, because the addition of 5/0.1 and 5/0.2 ZnO/CuNp increased the solubility of the adhesive, and therefore, zinc oxide and copper ions could diffuse and exert their combined cytotoxic effect. This increase in solubility can be explained by the presence of isopropanol, a highly water-soluble solvent in the adhesive composition [46]. However, Prime&Bond Active also showed increasing of the water sorption with the addition of ZnO/CuNp, because there probably is not

Table 4
Means and standard deviations of the water sorption ($\mu g/mm^3$) and solubility ($\mu g/mm^3$) after 28-day water storage obtained in each experimental condition (*).

ZnO/Cu concentration (%)	Prime&Bond Active		Ambar Universal	
	Water sorption	Solubility	Water sorption	Solubility
0 (control)	260.52 ± 16.09 ^{A}	92.82 ± 7.75 ^{a}	110.75 ± 9.93 A	140.19 ± 12.96 a
5 / 0.1	323.72 ± 43.30 ^{B}	99.05 ± 6.44 ^{a,b}	118.19 ± 8.76 A,B	71.12 ± 8.34 b
5 / 0.2	374.77 ± 22.66 ^{C}	107.01 ± 11.66 ^{b}	125.68 ± 8.68 B	73.27 ± 6.11 b

(*) Comparisons are valid only within column. Means identified with the same capital or lowercase letter, subscript or not subscripted letters are statistically similar. (Tukey´s test, $p \geq 0.05$).

Table 5
Means and standard deviations of the 24 h and 28-days Knoop microhardness (KHN) and degree of conversion (DC, %) obtained in each experimental condition (*).

ZnO/Cu concentration (%)	Prime&Bond Active			Ambar Universal		
	24 h KHN	28-days KHN	*in vitro* DC	24 h KHN	28-days KHN	*in vitro* DC
0 (control)	12.09 ± 0.22 ^{A}	14.49 ± 1.38 $_{A}$	69.61 ± 0.37 $_{a}$	8.02 ± 0.14 A	10.73 ± 0.60 a	92.06 ± 0.59 ^{a}
5 / 0.1	12.33 ± 0.25 ^{A}	14.45 ± 1.07 $_{A}$	71.28 ± 5.22 $_{a}$	13.24 ± 0.83 B	17.86 ± 0.77 b	95.74 ± 0.51 ^{b}
5 / 0.2	12.76 ± 1.31 ^{A}	14.15 ± 0.36 $_{A}$	71.48 ± 2.49 $_{a}$	16.71 ± 1.36 C	21.54 ± 0.54 c	95.82 ± 0.35 ^{b}

(*) Comparisons are valid only within adhesive and test. Means identified with the same capital or lowercase letter, subscript or not subscripted letters are statistically similar. (Tukey´s test, p ≥ 0.05).

a good chemical mixture between the nanoparticles and the adhesive components, increasing the water sorption and, consequently, the elution of some inadequately polymerized monomers and other resin components together with nanoparticles.

On the other hand, for Ambar Universal no significantly differences were observed in all groups in 0.01 v/v% dilution, and no differences in cytotoxicity were observed between the ZnO/CuNp concentrations and the control (commercial material), probably because the low water sorption and solubility that groups 5/0.1 and 5/0.2 presented with respect to the control, which means that the nanoparticles are not released so quickly, not producing a cytotoxic effect.

Several studies have shown that microhardness is increased when zinc or copper particles are incorporated in adhesive systems [18,47] because there could be a positive correlation between the volume fraction of filler and the microhardness of resin-based materials, since filler particles are harder than the organic phase of the material. In the case of Prime&Bond Active, the higher water sorption in 5/0.1 and 5/0.2 groups could be negatively influencing the effect of the ZnO/CuNp like filler particles on the microhardness, explaining the similar microhardness values between the ZnO/CuNp groups and the control. On the other hand, in Ambar Universal, ZnO/CuNp addition only slightly increase in the water sorption, which would allow the nanoparticles to increase the microhardness due to their effect as a filler. The same effect could occur for the degree of conversion, where the slight water sorption of 5/0.1 and 5/0.2 groups in Ambar Universal do not counteract the catalytic effect of copper, which may improve degrees of polymerization and dark reaction [48], increasing the *in vitro* and *in situ* degree of conversion in both adhesive strategies.

For both universal adhesive systems, all ZnO/CuNp groups showed similar values of resin-dentin bond strength, and a significantly decreased of the nanoleakage values for both adhesive strategies. Several hypotheses may help to understand nanoleakage results. Copper can increase the strength of the collagen network, one of the components of the hybrid layer, because the collagen cross-linking enzyme, lysyl oxidase (LOX), is copper dependent [49] and thus copper has an indirect effect as a cross-linking agent. Other study showed that, the

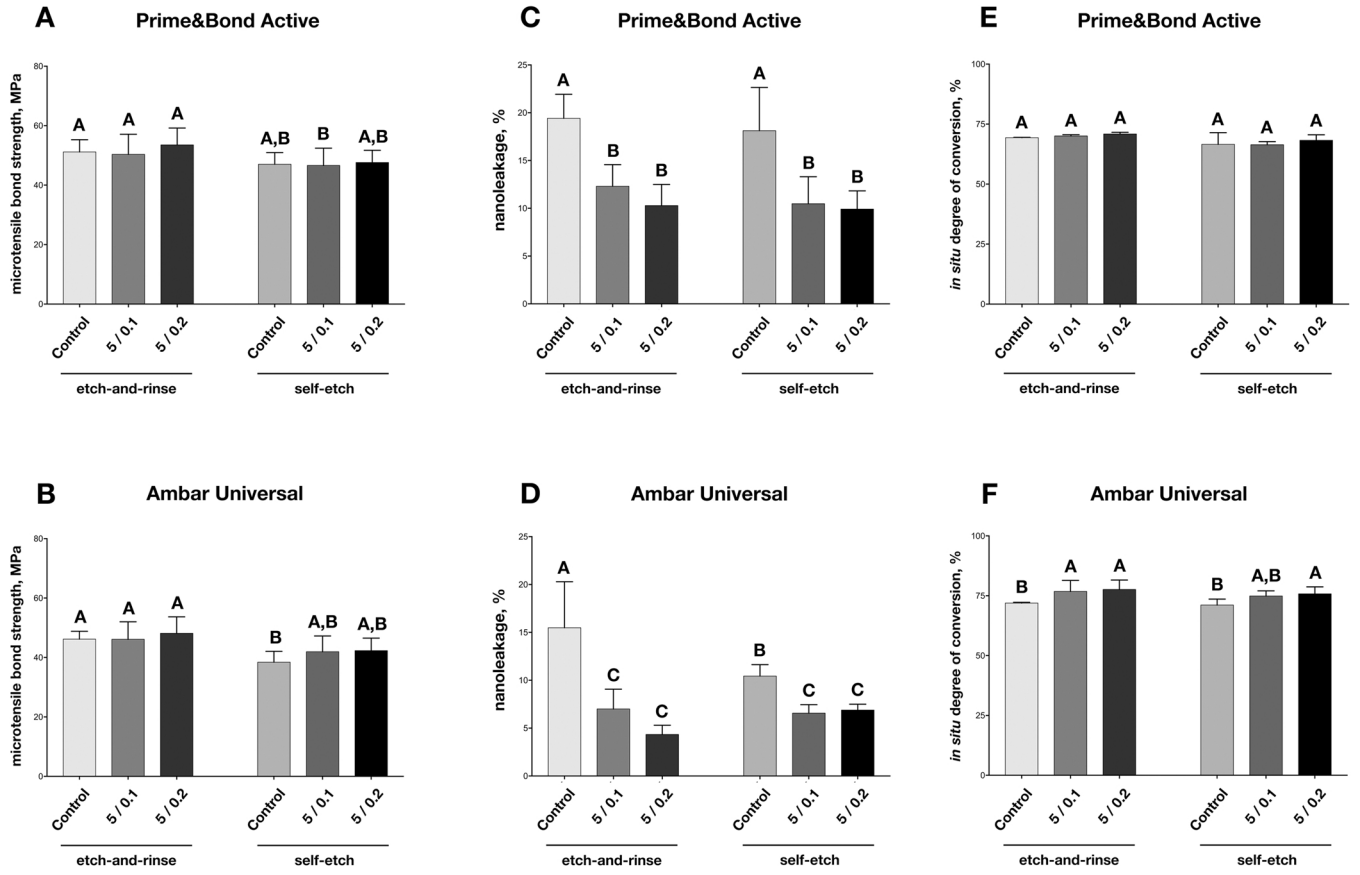

Fig. 4. Microtensile bond strength (A and B), nanoleakage (C and D) and *in situ* degree of conversion (E and F) of experimental adhesives containing zinc oxide and copper nanoparticles. Comparisons are valid only within test and adhesive. Mean ± SD were calculated. Means identified with the same letter are statistically similar. (Tukey´s test, p ≥ 0.05).

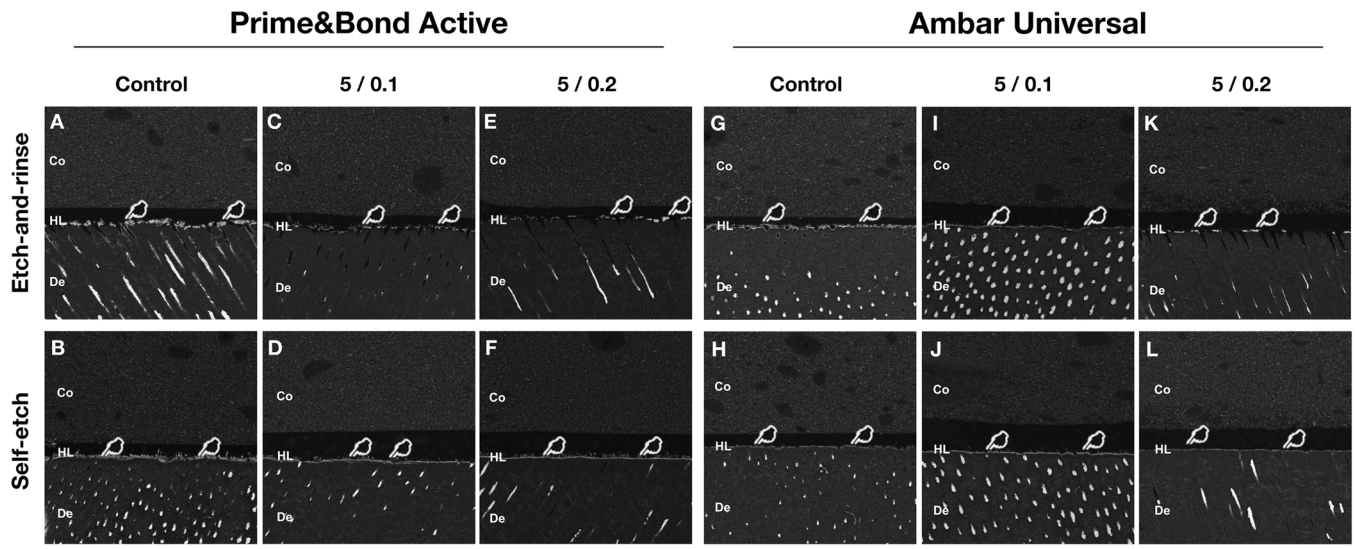

Fig. 5. Representative back-scattering SEM images of the resin–dentin interfaces bonded in the immediate time according to the different experimental conditions. (Co = composite; HL = hybrid layer and De = dentin).

incorporation of ZnO has resulted in the formation of apatite crystallites on the collagen fibrils, favoring dentin mineralization [21] and improved the cross-linking effect. This cross-linker action of both nanoparticles alone may increase the resistance of collagen, leaving it less susceptible to the effects of proteolytic enzymes such as MMPs and CTs, indirectly decreasing the immediate nanoleakage, as well as previously showed by adhesive-containing CuNp [18,19] and Zn alone [50]. However, further studies are still required to evaluate the effect of ZnONp and CuNp on these enzymes, and to its effect as a cross-linking agent. In addition, studies are still required to evaluate their effects on host-derived proteases and to evaluate whether or not ZnO/CuNp-containing adhesive interfaces are less prone to degradation under oral conditions and in more challenging conditions such in a cariogenic environment.

5. Conclusion

The present study was capable to demonstrate that the addition of zinc oxide and copper nanoparticles to universal adhesive systems in concentrations up to 5/0.2 wt% is a feasible approach to provide them with antimicrobial properties, as well as to improve and stabilize the resin-dentin interface, with no significantly biological hazards. The zinc oxide and copper nanoparticles addition have an influence on the mechanical properties dependent on the adhesive system, so a good knowledge of the composition of the adhesive is necessary, to produce a universal adhesive system incorporating these nanoparticles for commercial use.

Conflict of interest

The authors declare no competing financial interest.

Acknowledgment

This study was performed by Mario Felipe Gutiérrez Reyes as partial fulfillment of his PhD degree at the State University of Ponta Grossa (UEPG), Ponta Grossa, PR, Brazil. This project was supported by Fondecyt (Fondo Nacional de Desarrollo Científico y Tecnológico - Chile) project 1170575 (Chile; EF). Also, this study was partially supported by the National Council for Scientific and Technological Development (CNPq) under grants 305588/2014-1 (Brazil; ADL) and in part by the Coordenação de Aperfeiçoamento de Pessoal de Nível Superior - Brasil (CAPES) - Finance Code 001. The corresponding author dedicates this article to his two kids, Elisa and Eduardo, for their enormous inspiration.

References

[1] G.J. Christensen, Should resin-based composite dominate restorative dentistry today? J. Am. Dent. Assoc. 141 (2010) 1490–1493, https://doi.org/10.14219/jada.archive.2010.0112.
[2] A. Astvaldsdottir, J. Dagerhamn, J.W. van Dijken, A. Naimi-Akbar, G. Sandborgh-Englund, S. Tranaeus, M. Nilsson, Longevity of posterior resin composite restorations in adults - a systematic review, J. Dent. 43 (2015) 934–954, https://doi.org/10.1016/j.jdent.2015.05.001.
[3] P. Spencer, Q. Ye, J. Park, E.M. Topp, A. Misra, O. Marangos, Y. Wang, B.S. Bohaty, V. Singh, F. Sene, J. Eslick, K. Camarda, J.L. Katz, Adhesive/Dentin interface: the weak link in the composite restoration, Ann. Biomed. Eng. 38 (2010) 1989–2003, https://doi.org/10.1007/s10439-010-9969-6.
[4] A.R. Hunter, E.T. Treasure, A.J. Hunter, Increases in cavity volume associated with the removal of class 2 amalgam and composite restorations, Oper. Dent. 20 (1995) 2–6.
[5] V. Deligeorgi, I. Mjör, N. Wilson, An overview of reasons for the placement and replacement of restorations, Prim. Dent. Care 8 (2001) 5–11, https://doi.org/10.1308/135576101771799335.
[6] I.A. Mjor, J.E. Moorhead, J.E. Dahl, Reasons for replacement of restorations in permanent teeth in general dental practice, Int. Dent. J. 50 (2000) 361–366, https://doi.org/10.1111/j.1875-595X.2000.tb00569.x.
[7] P. Spencer, Q.Y. Jonggu Park, A. Misra, B.S. Bohaty, V. Singh, R. Parthasarathy, F. Sene, S.E. de Paiva Goncalves, J. Laurence, Durable bonds at the adhesive/dentin interface: an impossible mission or simply a moving target? Braz. Dent. Sci. 15 (2012) 4–18.
[8] M.R. Carrilho, F.R. Tay, A.M. Donnelly, K.A. Agee, L. Tjaderhane, A. Mazzoni, L. Breschi, S. Foulger, D.H. Pashley, Host-derived loss of dentin matrix stiffness associated with solubilization of collagen, J. Biomed. Mater. Res. B Appl. Biomater. 90 (2009) 373–380, https://doi.org/10.1002/jbm.b.31295.
[9] F. Femiano, R. Femiano, L. Femiano, A. Jamilian, R. Rullo, L. Perillo, Dentin caries progression and the role of metalloproteinases: an update, Eur. J. Paediatr. Dent. 17 (2016) 243–247.
[10] L. Tjaderhane, M.A. Buzalaf, M. Carrilho, C. Chaussain, Matrix metalloproteinases and other matrix proteinases in relation to cariology: the era of' dentin degradomics', Caries Res. 49 (2015) 193–208, https://doi.org/10.1159/000363582.
[11] L. Chen, H. Shen, B.I. Suh, Antibacterial dental restorative materials: a state-of-the-art review, Am. J. Dent. 25 (2012) 337–346.
[12] S. Imazato, S. Ma, J.H. Chen, H.H. Xu, Therapeutic polymers for dental adhesives: loading resins with bio-active components, Dent. Mater. 30 (2014) 97–104, https://doi.org/10.1016/j.dental.2013.06.003.
[13] H. Palza, Antimicrobial polymers with metal nanoparticles, Int. J. Mol. Sci. 16 (2015) 2099–2116, https://doi.org/10.3390/ijms16012099.
[14] A.M. Schrand, M.F. Rahman, S.M. Hussain, J.J. Schlager, D.A. Smith, A.F. Syed, Metal-based nanoparticles and their toxicity assessment, Wiley Interdiscip. Rev. Nanomed. Nanobiotechnol. 2 (2010) 544–568, https://doi.org/10.1002/wnan.103.
[15] A.P. de Souza, R.F. Gerlach, S.R. Line, Inhibition of human gingival gelatinases (MMP-2 and MMP-9) by metal salts, Dent. Mater. 16 (2000) 103–108, https://doi.org/10.1016/S0109-5641(99)00084-6.
[16] A. Simeon, H. Emonard, W. Hornebeck, F.X. Maquart, The tripeptide-copper complex glycyl-L-histidyl-L-lysine-Cu2+ stimulates matrix metalloproteinase-2

expression by fibroblast cultures, Life Sci. 67 (2000) 2257–2265, https://doi.org/10.1016/S0024-3205(00)00803-1.
[17] M. Toledano, M. Yamauti, M.E. Ruiz-Requena, R. Osorio, A ZnO-doped adhesive reduced collagen degradation favouring dentine remineralization, J. Dent. 40 (2012) 756–765, https://doi.org/10.1016/j.jdent.2012.05.007.
[18] M.F. Gutierrez, P. Malaquias, V. Hass, T.P. Matos, L. Lourenco, A. Reis, A.D. Loguercio, P.V. Farago, The role of copper nanoparticles in an etch-and-rinse adhesive on antimicrobial activity, mechanical properties and the durability of resin-dentine interfaces, J. Dent. 61 (2017) 12–20, https://doi.org/10.1016/j.jdent.2017.04.007.
[19] M.F. Gutierrez, P. Malaquias, T.P. Matos, A. Szesz, S. Souza, J. Bermudez, A. Reis, A.D. Loguercio, P.V. Farago, Mechanical and microbiological properties and drug release modeling of an etch-and-rinse adhesive containing copper nanoparticles, Dent. Mater. 33 (2017) 309–320, https://doi.org/10.1016/j.dental.2016.12.011.
[20] D.C. Barcellos, B.M. Fonseca, C.R. Pucci, B. Cavalcanti, S. Persici Ede, S.E. Goncalves, Zn-doped etch-and-rinse model dentin adhesives: dentin bond integrity, biocompatibility, and properties, Dent. Mater. 32 (2016) 940–950, https://doi.org/10.1016/j.dental.2016.04.003.
[21] M. Toledano, S. Sauro, I. Cabello, T. Watson, R. Osorio, A Zn-doped etch-and-rinse adhesive may improve the mechanical properties and the integrity at the bonded-dentin interface, Dent. Mater. 29 (2013) e142–52, https://doi.org/10.1016/j.dental.2013.04.024.
[22] T. Takatsuka, K. Tanaka, Y. Iijima, Inhibition of dentine demineralization by zinc oxide: in vitro and in situ studies, Dent. Mater. 21 (2005) 1170–1177, https://doi.org/10.1016/j.dental.2005.02.006.
[23] R.J. Lynch, D. Churchley, A. Butler, S. Kearns, G.V. Thomas, T.C. Badrock, L. Cooper, S.M. Higham, Effects of zinc and fluoride on the remineralisation of artificial carious lesions under simulated plaque fluid conditions, Caries Res. 45 (2011) 313–322, https://doi.org/10.1159/000324804.
[24] R. Huang, M. Li, R.L. Gregory, Effect of nicotine on growth and metabolism of Streptococcus mutans, Eur. J. Oral Sci. 120 (2012) 319–325, https://doi.org/10.1111/j.1600-0722.2012.00971.x.
[25] D. Kraus, M. Wolfgarten, N. Enkling, E.H. Helfgen, M. Frentzen, R. Probstmeier, J. Winter, H. Stark, In-vitro cytocompatibility of dental resin monomers on osteoblast-like cells, J. Dent. 65 (2017) 76–82, https://doi.org/10.1016/j.jdent.2017.07.008.
[26] ISO, International Organization for Standardization 4049. Dentistry: Resin Based Dental Fillings, International Organization for Standardization, Geneva, Switzerland, 2000.
[27] C.A. Schneider, W.S. Rasband, K.W. Eliceiri, NIH Image to ImageJ: 25 years of image analysis, Nat. Methods 9 (2012) 671–675.
[28] J.F. Hernandez-Sierra, F. Ruiz, D.C. Pena, F. Martinez-Gutierrez, A.E. Martinez, J. Guillen Ade, H. Tapia-Perez, G.M. Castanon, The antimicrobial sensitivity of Streptococcus mutans to nanoparticles of silver, zinc oxide, and gold, Nanomedicine 4 (2008) 237–240, https://doi.org/10.1016/j.nano.2008.04.005.
[29] M. Amiri, Z. Etemadifar, A. Daneshkazemi, M. Nateghi, Antimicrobial effect of copper oxide nanoparticles on some oral Bacteria and Candida species, J. Dent. Biomater. 4 (2017) 347–352.
[30] X. Wang, S. Liu, M. Li, P. Yu, X. Chu, L. Li, G. Tan, Y. Wang, X. Chen, Y. Zhang, C. Ning, The synergistic antibacterial activity and mechanism of multicomponent metal ions-containing aqueous solutions against Staphylococcus aureus, J. Inorg. Biochem. 163 (2016) 214–220, https://doi.org/10.1016/j.jinorgbio.2016.07.019.
[31] M. Saffarpour, M. Rahmani, M. Tahriri, A. Peymani, Antimicrobial and bond strength properties of a dental adhesive containing zinc oxide nanoparticles, Braz. J. Oral Sci. 15 (2016) 66–69, https://doi.org/10.20396/bjos.v15i1.8647127.
[32] S.M. Dizaj, F. Lotfipour, M. Barzegar-Jalali, M.H. Zarrintan, K. Adibkia, Antimicrobial activity of the metals and metal oxide nanoparticles, Mater. Sci. Eng. C Mater. Biol. Appl. 44 (2014) 278–284, https://doi.org/10.1016/j.msec.2014.08.031.
[33] A. Raghunath, E. Perumal, Metal oxide nanoparticles as antimicrobial agents: a promise for the future, Int. J. Antimicrob. Agents 49 (2017) 137–152, https://doi.org/10.1016/j.ijantimicag.2016.11.011.
[34] M. Heinlaan, A. Ivask, I. Blinova, H.C. Dubourguier, A. Kahru, Toxicity of nanosized and bulk ZnO, CuO and TiO2 to bacteria Vibrio fischeri and crustaceans Daphnia magna and Thamnocephalus platyurus, Chemosphere 71 (2008) 1308–1316, https://doi.org/10.1016/j.chemosphere.2007.11.047.
[35] S. Sabella, R.P. Carney, V. Brunetti, M.A. Malvindi, N. Al-Juffali, G. Vecchio, S.M. Janes, O.M. Bakr, R. Cingolani, F. Stellacci, P.P. Pompa, A general mechanism for intracellular toxicity of metal-containing nanoparticles, Nanoscale 6 (2014) 7052–7061, https://doi.org/10.1039/c4nr01234h.
[36] S.R. Saptarshi, A. Duschl, A.L. Lopata, Biological reactivity of zinc oxide nanoparticles with mammalian test systems: an overview, Nanomedicine (Lond.) 10 (2015) 2075–2092, https://doi.org/10.2217/nnm.15.44.
[37] S. Seker, A.E. Elcin, T. Yumak, A. Sinag, Y.M. Elcin, In vitro cytotoxicity of hydrothermally synthesized ZnO nanoparticles on human periodontal ligament fibroblast and mouse dermal fibroblast cells, Toxicol. In Vitro 28 (2014) 1349–1358, https://doi.org/10.1016/j.tiv.2014.06.016.
[38] A.P. Ingle, N. Duran, M. Rai, Bioactivity, mechanism of action, and cytotoxicity of copper-based nanoparticles: a review, Appl. Microbiol. Biotechnol. 98 (2014) 1001–1009, https://doi.org/10.1007/s00253-013-5422-8.
[39] Y. Wang, X.Y. Zi, J. Su, H.X. Zhang, X.R. Zhang, H.Y. Zhu, J.X. Li, M. Yin, F. Yang, Y.P. Hu, Cuprous oxide nanoparticles selectively induce apoptosis of tumor cells, Int. J. Nanomedicine 7 (2012) 2641–2652, https://doi.org/10.2147/ijn.s31133.
[40] L. Li, M.L. Fernandez-Cruz, M. Connolly, E. Conde, M. Fernandez, M. Schuster, J.M. Navas, The potentiation effect makes the difference: non-toxic concentrations of ZnO nanoparticles enhance Cu nanoparticle toxicity in vitro, Sci. Total Environ. 505 (2015) 253–260, https://doi.org/10.1016/j.scitotenv.2014.10.020.
[41] E.A. Koulaouzidou, M. Helvatjoglu-Antoniades, G. Palaghias, A. Karanika-Kouma, D. Antoniades, Cytotoxicity of dental adhesives in vitro, Eur. J. Dent. 3 (2009) 3–9.
[42] A. Sengun, M. Yalcin, H.E. Ulker, B. Ozturk, S.S. Hakki, Cytotoxicity evaluation of dentin bonding agents by dentin barrier test on 3-dimensional pulp cells, Oral Surg. Oral Med. Oral Pathol. Oral Radiol. Endod. 112 (2011) e83–8, https://doi.org/10.1016/j.tripleo.2011.02.023.
[43] S. Ratanasathien, J.C. Wataha, C.T. Hanks, J.B. Dennison, Cytotoxic interactive effects of dentin bonding components on mouse fibroblasts, J. Dent. Res. 74 (1995) 1602–1606, https://doi.org/10.1177/00220345950740091601.
[44] E.C. Kim, H. Park, S.I. Lee, S.Y. Kim, Effect of the acidic dental resin monomer 10-methacryloyloxydecyl dihydrogen phosphate on odontoblastic differentiation of human dental pulp cells, Basic Clin. Pharmacol. Toxicol. 117 (2015) 340–349, https://doi.org/10.1111/bcpt.12404.
[45] ISO, International Organization for Standardization 10993-5:2009 Biological Evaluation of Medical Devices – Part 5: Tests for in Vitro Cytotoxicity, (2009), pp. 1–34.
[46] Dentsply Sirona FAQs, https://www.dentsplysirona.com/content/dam/dentsply/pim/manufacturer/Restorative/Direct_Restoration/Adhesives/Universal_Adhesives/PrimeBond_active/PrimeBond%20active_Scientific%20Compendium_EN.pdf (Accessed 20 July 2017).
[47] C. Pomacondor-Hernandez, R. Osorio, F.S. Aguilera, I. Cabello, M. De Goes, M. Toledano, Effect of zinc-doping in physicochemical properties of dental adhesives, Am. J. Dent. 28 (2015) 292–296.
[48] H.B. Song, N. Sowan, P.K. Shah, A. Baranek, A. Flores, J.W. Stansbury, C.N. Bowman, Reduced shrinkage stress via photo-initiated copper(I)-catalyzed cycloaddition polymerizations of azide-alkyne resins, Dent. Mater. 32 (2016) 1332–1342, https://doi.org/10.1016/j.dental.2016.07.014.
[49] B. Marelli, D. Le Nihouannen, S.A. Hacking, S. Tran, J. Li, M. Murshed, C.J. Doillon, C.E. Ghezzi, Y.L. Zhang, S.N. Nazhat, J.E. Barralet, Newly identified interfibrillar collagen crosslinking suppresses cell proliferation and remodelling, Biomaterials 54 (2015) 126–135, https://doi.org/10.1016/j.biomaterials.2015.03.018.
[50] G.S. Almeida, E.M. da Silva, J.G.A. Guimaraes, R.N.L. da Silva, G.B. Dos Santos, L.T. Poskus, ZnCl2 incorporated into experimental adhesives: selected physicochemical properties and resin-dentin bonding stability, Biomed Res. Int. 2017 (2017) 5940479, , https://doi.org/10.1155/2017/5940479.